Catalysis Today 157 (2010) 462–466

Contents lists available at ScienceDirect

Catalysis Today

journal homepage: www.elsevier.com/locate/cattod

Catalytic production of methane from CO_2 and H_2 at low temperature: Insight on the reaction mechanism

Marc Jacquemin*, Antoine Beuls, Patricio Ruiz

Université catholique de Louvain, Institute of Condensed Matter and Nanosciences - IMCN, Division "MOlecules, Solids and reactiviTy – MOST"[1], Croix du Sud 2/17, B-1348 Louvain-la-Neuve, Belgium

ARTICLE INFO

Article history:
Available online 16 July 2010

Keywords:
CO_2
Methanation
Dissociation
DRIFT spectroscopy

ABSTRACT

Experimental evidences show that it is possible to produce methane from an exclusively inorganic way using CO_2 and H_2 on a $Rh/\gamma\text{-}Al_2O_3$ catalyst at low temperature and atmospheric pressure. New insights on the mechanism of methanation are given. The first step of the mechanism in the methanation reaction could be the chemisorption of CO_2 on the catalyst. The second step is the dissociation of CO_2 into CO and O adsorbed on the surface. The third step is the reaction of dissociated species with H_2. Adsorption, dissociation of CO_2 and the reaction of dissociated species with H_2 are evidenced by *in situ* DRIFT experiments. The reaction could occur between the adsorbed species. However a reaction between adsorbed species and gaseous hydrogen cannot be excluded. XPS shows that the CO_2 oxidizes the catalyst and this oxidation deactivates the catalyst. The conversion of CO_2 also increases with temperature. Methane is the unique hydrocarbon molecule formed and obtained with almost 100% selectivity. No other hydrocarbonated products have been observed.

1. Introduction

The atmospheric CO_2 concentration is continuously and significantly increasing. This is principally due to the high consumption of carbon-based energy and low efficiency of energetic processes. It is estimated that during the 21st century, the minimal amount of CO_2 emitted could be higher than 3480 Gt. For comparison, between 1850 and 2000, the amount of CO_2 emitted was only 1100 Gt [1]. Therefore, there is a worldwide interest for reducing the CO_2 emissions. The reduction of the CO_2 atmospheric concentration is a topical need and a real challenge for the scientific community.

Nowadays, great efforts are made to eliminate or transform the carbon dioxide which participates consistently to the greenhouse gas emissions. Two main solutions are proposed: (i) to capture CO_2 at its source and store it in the geological subsurface where it will no longer be able to contribute to the global warming [2,3], (ii) to promote the transformation of CO_2 in the presence of an adequate catalyst at high temperature [4,5]. However the first solution has some major drawbacks such as the high cost, the problem of the transport of CO_2 and also the risks of gas leakage in the atmosphere. The main criticisms towards the high temperature processes are the high necessity for energy and the low selectivity of the reactions. Some examples of these high temperature reactions are (i) the hydrogenation of CO_2 which generally leads to the formation of methanol with a reaction temperature ranging between 573 and 773 K on Fe or Ni-based catalysts [6,7]; (ii) the catalytic reaction between carbon dioxide and methane (373–573 K) [8]; (iii) the use of CO_2 as an oxidant, such as in the oxidation of ethylbenzene with $K_2O/TiO_2–ZrO_2$ catalyst at 873 K [9] and (iv) the dry reforming, which is the reaction between carbon dioxide and aliphatic hydrocarbons to produce a mix of H_2/CO on Rh or Ni-based catalysts between 973 and 1123 K. The main problem of dry reforming is the deactivation caused by coke formation during methane decomposition [4,10]. Actually, no sustainable solution is proposed to avoid the rejection of CO_2 in the atmosphere.

CO_2 is a stable molecule. Both terms of the Gibbs free energy disadvantage the conversion of CO_2 into other products. The C=O bonds in CO_2 molecules are quite stable and an important energy input (heat) must be supplied to make their dissociation possible. For the $CO_{2(g)} \rightarrow CO_{(g)} + (1/2)O_{2(g)}$ reaction, at the atmospheric pressure and 298 K, the ΔH is about 293 kJ/mol CO_2. The entropy term in the free energy (ΔG) is not favourable because CO_2 is a small gaseous molecule. At 573 K, ΔG is 256 kJ/mol. To give an example of the stability of CO_2, it is estimated that at 2273 K [11] not more than 2% of CO_2 transforms into $CO_{(g)}$ and $O_{2(g)}$. The transformation of CO_2 is more energy-demanding when CO_2 is used as

---

* Corresponding author. Tel.: +32 10473597; fax: +32 10473649.
E-mail addresses: marc.jacquemin@uclouvain.be (M. Jacquemin), patricio.ruiz@uclouvain.be (P. Ruiz).

[1] IMCN and MOST are new research entities involving the group formerly known as "Unité de catalyse et chimie des matériaux divisés".

0920-5861/$ – see front matter © 2010 Elsevier B.V. All rights reserved.
doi:10.1016/j.cattod.2010.06.016

a single reactant. The reaction is thermodynamically easier if CO_2 is used as a co-reactant with other substances with a higher Gibbs free energy, such as H_2. For the $CO_2 + 4H_2 = CH_4 + 2H_2O$ reaction, the enthalpy is about $\Delta H^\circ = -167$ kJ/mol. This reaction is reversible and exothermic.

Recent experiments have demonstrated that CO_2 can react with H_2 in the presence of Rh/γ-Al_2O_3 to produce methane at low (room) temperature and atmospheric pressure [12]. These results show that the recycling of CO_2 to produce methane (chemicals), under friendly conditions (room temperature and atmospheric pressure), could be possible in the near future. The produced methane can be injected in petrochemical and/or chemical industries. The only energy-consuming step is H_2 production. The major part of H_2 is currently produced by steam reforming [4] but it could also be produced from environment-friendly processes and renewable energy sources such as wind turbines, photovoltaic cells or solar panels, barrage electricity generator, etc. [13].

However, the transformation of CO_2 at low temperature and atmospheric pressure with a high selectivity is a new challenge. Insight on the reaction mechanism is necessary to optimize the process and improve the performances. This is the main objective of this work using DRIFT experiments. A study of the reaction temperature has also been done in this paper.

2. Experimental

2.1. Preparation of the catalyst

A Rh/γ-Al_2O_3 catalyst was prepared by wet impregnation of alumina with a solution of $(NH_4)_3RhCl_6{\cdot}3H_2O$. 4 g of γ-$Al_2O_3$ (Alfa Aesar, 39812) was dipped in 400 ml of distilled water. $(NH_4)_3RhCl_6{\cdot}3H_2O$ (Acros, 195510010) was added to obtain 1% by weight of Rhodium. The solution was mixed at 293 K for 3 h under magnetic stirring. Water was removed by evaporation under reduced pressure in a rotavapor at 313 K. Then, the solid was dried at 383 K for 12 h and calcined at 973 K for 4 h in a furnace under static air.

2.2. Characterization

The chemical composition of catalysts was determined by Inductively Coupled Plasma Atomic Emission Spectroscopy (ICP-AES) on an Iris Advantage equipment from Jarrel Ash Corporation. The catalyst was dried at 383 K before measurement.

Textural analysis of the catalyst was carried out on a Micromeritics ASAP 2000/2010 equipment using N_2 adsorption/desorption at liquid N_2 temperature, working with P/P_0 pressures in the range of 10^{-2} to 1.0. Before the measurements, 150 mg of the samples were degassed at 423 K overnight under a 50 mTorr vacuum. BET and BJH equations were used to determine surface area, porous volume and pore size distribution.

X-ray diffraction (XRD) analyses were performed on the fresh catalyst on a Siemens D5000 diffractometer using the Kα radiation of Cu (λ = 1.5418 Å). The 2θ range was scanned between 10° and 90° by steps of 0.02° with an acquisition time of 2 s at each step. Identification of the phases was carried out using the ICDD-JCPDS database.

Surface characterization was done by X-ray photoelectron spectroscopy (XPS) measurements on a Kratos Axis Ultra spectrometer (Kratos Analytical – Manchester – UK) equipped with a monochromatised aluminium X-ray source (powered at 10 mA and 15 kV). The experiment was carried out on the freshly prepared catalyst and on the same sample after the reduction step and after the reaction. The sample powders were pressed into small stainless steel troughs mounted on a multi specimen holder. The pressure in the analysis chamber was around 10^{-6} Pa. The angle between the normal to the sample surface and the lens was 55°. The analyzed area was 700 μm × 300 μm. The pass energy of the hemispherical analyser was set at 40 eV. Charge stabilisation was achieved by using the Kratos Axis device. The electron source was operated at a filament current of 1.8 A and a bias of −1.1 eV. The following sequence of spectra was recorded: survey spectrum, C 1s, O 1s, Al 2p and Rh 3d and C 1s again to check the stability of charge compensation in function of time and the absence of degradation of the sample during the analyses. The binding energy (BE) values were referred to the $\underline{C}$-(C, H) component of the C 1s peak fixed at 284.8 eV. The spectra were decomposed with the CasaXPS program (Casa Software Ltd., UK) with a Gaussian/Lorentzian (70/30) product function. Molar fractions were calculated using peak areas normalised on the basis of acquisition parameters, sensitivity factors and transmission factors provided by the manufacturer.

CO_2 chemisorption measurements were performed on a Micromeritics ASAP2010Chemi apparatus. The U-shaped sample tube containing 150 mg of the catalyst was first flushed under a H_2 flow at 623 K for 1 h to reduce the catalyst except for the measurement of the non-reduced catalyst for which a flow of He was used in the same conditions. Then, the sample was flushed with a He flow at 298 K for 2 h. Finally the sample was evacuated at 298 K for 2 h down to a residual pressure of <5 μmHg. A first CO_2 adsorption isotherm was recorded at 298 K. Then the sample was evacuated at the same temperature and a second CO_2 adsorption isotherm was measured. The difference between the two isotherms corresponds to the amount of carbon dioxide chemisorbed on the samples at 298 K. The results were expressed in terms of cm^3 of chemisorbed CO_2 per gram of catalyst.

Dispersion of Rh on γ-Al_2O_3 was determined by hydrogen chemisorption. Experiments were conducted at 298 K using a Micromeritics ASAP2010Chemi apparatus. The sample (150 mg) was first degassed under vacuum down to <5 μmHg. Then, it was reduced at 623 K under a pure flow of Hydrogen (Praxair, 99.999%) for 1 h and then flushed for 2 h under He and finally cooled down to 298 K. The samples were evacuated at 298 K for 2 h down to a residual pressure of <5 μmHg. A first H_2 adsorption isotherm was recorded at 298 K. Then the sample was evacuated at the same temperature and a second H_2 adsorption isotherm was measured. The difference between the two isotherms corresponds to the amount of hydrogen chemisorbed on the samples at 298 K. These values were used to estimate the dispersion assuming a 1:1 ratio between the chemisorbed gas atoms and the active metal atoms (1 H_2 molecule for 2 Rh atoms) [14,15].

2.3. Catalytic test

The catalyst was sieved between 200 and 315 μm. 150 mg of catalysts were introduced on the frit of a quartz reactor of 8 mm internal diameter located inside an electrically heated furnace. The temperature was checked with a thermocouple located inside a quartz thermo well fixed into the catalytic bed.

The first step of the catalytic test was the reduction of the catalyst under a flow of pure H_2 at 623 K for 1 h and cooling down until the temperature of the catalytic test under H_2: 298 K or 373 K or 423 K. Then a known quantity of carbon dioxide carried with He was introduced in the reactor with a molar ratio of 1:1, the flow rate of the gas was 20 ml/min during 30 min. The next step of the catalytic test was the injection of pure H_2 on the catalyst (20 ml/min). Several cycles of the last two steps (successive introduction of CO_2 and H_2) have been done. An important feature of the experiments is that they were performed at low temperature and atmospheric pressure. Reactants and products were monitored by a quadrupole mass spectrometer (Balzers QMS 200).

Table 1
Production of methane feeding the reactor with different amounts of CO_2 and at different temperatures.

Temperature (K)	Quantity of CO_2 introduced (mmol)	Conversion (%)	Quantity of CH_4 produced (mmol)	Quantity of CH_4 produced ($mol_{CH_4}\ mol^{-1}_{Rh(s)}\ h^{-1}$)[a]
298[b]	1.33	0	0	0
298	1.33	0.63	0.0838	2.1
298	0.0417	17	0.0071	34.5
373	0.0417	19	0.0079	39.0
423	0.0417	21	0.0088	42.4

[a] Moles of CH_4 produced by moles of Rh on the surface (calculated with the dispersion) by hour.
[b] Unreduced catalyst.

The evolution of CO_2 adsorption with time and the reaction with H_2 were also followed by *in situ* diffuse reflectance infrared Fourier transform spectroscopy (DRIFTS) on the neat catalyst. Spectra were collected on a Brücker Equinox 55 infrared spectrometer equipped with an air-cooled MIR source with KBr optics and a MCT detector. Spectra were obtained by collecting 200 scans with a resolution of 4 cm^{-1} and are presented in absorbance mode without any manipulation. Samples were placed inside a commercial *in situ* cell (Spectra-Tech 0030-102) with ZnSe windows. The background was collected by replacing the catalyst by a mirror in the cell and this last one was flushed with He for 15 min (20 ml/min) to remove CO and CO_2 which are present in the atmosphere. The first step of the catalytic test was the reduction of the solid under a flow of pure H_2 at 623 K for 1 h followed by cooling down to room temperature under the same H_2 flow. Then, a known quantity of carbon dioxide (1.33 mmol) carried with He was introduced in the reactor and finally hydrogen was introduced into the cell during 15 min with a flow rate of 20 ml/min. Other experiments were also done in which CO_2 was replaced by CO.

3. Results

3.1. Production of methane

Fig. 1 shows a typical result during catalytic tests on the Rh/γ-Al_2O_3 at 298 K. In the first step, the catalyst was reduced for 1 h under H_2 at 623 K. The catalyst was allowed to cool down to 298 K under the H_2 flow. The graph is taken just when the temperature of the catalytic test was reached. After H_2 flushing for 10 min at room temperature, a known quantity of CO_2 was introduced (1.33 mmol). At this moment, an increase of a number of masses was observed in MS but for the clarity, only mass 15 was presented, which is a characteristic fragment of CH_4. The second curve in Fig. 1 corresponds to the “blank”, namely a catalytic test performed without catalyst but in the presence of glass beads. In this case, the curve stayed flat indicating that there is no production of methane. On the contrary, in the presence of the catalyst, mass 15 increases indicating that methane was effectively produced. Similar results have been obtained with the other fragments of methane. Water was not observed during the reaction. A deactivation was observed in the third cycle of the reaction test.

Table 1 presents a typical result obtained during catalytic tests on Rh/γ-Al_2O_3 when two different amounts of CO_2 (1.33 and 0.0417 mmol) were introduced in the reactor. The main observation from these results is that the production of CH_4 was higher when very small amounts of CO_2 were flushed. Different reaction temperatures have also been studied (298, 373 and 423 K). The conversion increases weakly with the temperature. As indicated previously, the results confirm that at all temperatures studied, no other hydrocarbon products have been detected. The only product of the reaction is methane [12]. Calculations show that the selectivity is about 100% at all temperatures.

DRIFT results are presented in Fig. 2. After introduction of CO_2, some bands are present showing an interaction between rhodium and CO. The band at 2048 cm^{-1} corresponds to linear Rh–CO [16]. The band at 2123 cm^{-1} is attributed to the interaction between an oxidized rhodium atom (Rh^{3+}) [17] and CO. Bands at 2024 and 2092 cm^{-1} correspond to gem-dicarbonyl Rh–$(CO)_2$ [16]. The presence of these bands demonstrates the dissociation of CO_2 on the catalyst surface. They are modified in the presence of hydrogen: bands at 2123, 2092 and 2024 cm^{-1} decrease or disappear, showing that H_2 reacts with the dissociated CO_2 species. The bands of the linear Rh-CO and gem-dicarbonyl Rh–$(CO)_2$ are still present when CO is adsorbed on the surface of the catalyst indicating that CO_2 is really dissociated into CO.

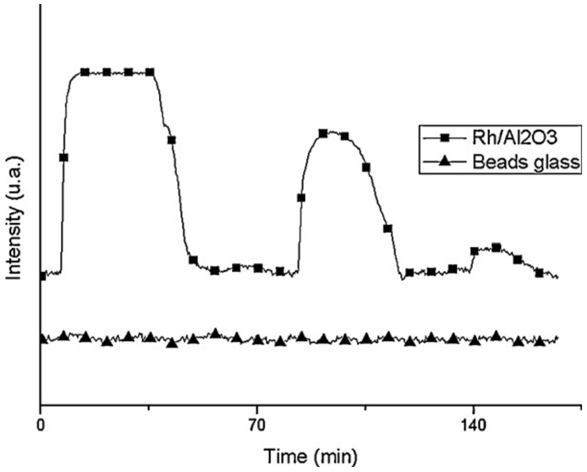

Fig. 1. Catalytic test on the Rh-γAl_2O_3 at 298 K. The masses were followed in continuous with a MS. *Y*-axis represents the intensity (arbitrary units) and the *X*-axis the time.

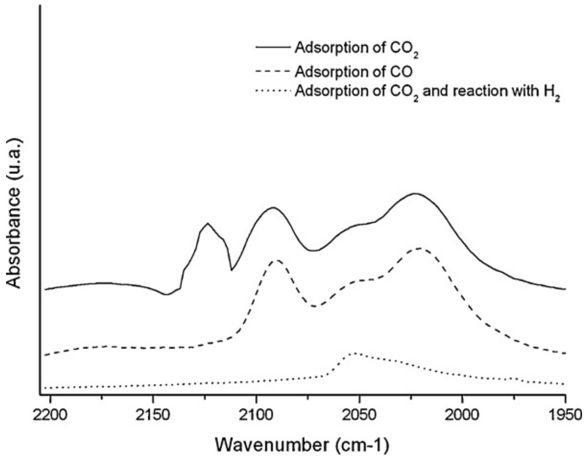

Fig. 2. DRIFT results after adsorption of CO_2 and CO and after adsorption of CO_2 and reaction with hydrogen.

Table 2
Experimental loading and textural analysis of the support and catalyst.

	Rh (%)	S_{BET} (m^2/g)	*D* pore (Å)	*V* pore (cm^3/g)
γ-Al_2O_3	–	54	129	0.2
Rh/γ-Al_2O_3	1	59	180	0.3

3.2. Catalyst characterization

The experimental loading of rhodium on the support has been checked by ICP-AES (Table 2): the rhodium content is 1%. No difference of specific surface area and porous volume has been measured between the support and the catalyst. The pore size distribution shows that the samples are mesoporous.

In XRD experiments, only the crystalline patterns of γ-Al_2O_3 (JCPDS 48-0367) were detected. No trace of crystalline pattern of Rh or Rh_2O_3 was detected during the analysis on the fresh catalyst.

Rh dispersion on the support determined through H_2 chemisorption analysis is about 28%.

XPS results are presented in Table 3. For the fresh Rh/γ-Al_2O_3, the binding energies values of the Al 2p and O 1s peaks correspond to values assigned to γ-Al_2O_3. The binding energy of Rh $3d_{5/2}$ corresponds to Rh_2O_3. After reduction in H_2, the binding energy of the Rh $3d_{5/2}$ orbital decreases, indicating that rhodium gets reduced. The binding energy of the Rh $3d_{5/2}$ peak seems to increase after introduction of CO_2 which indicates that rhodium was oxidized during the reaction. The binding energies of Al 2p and O 1s peaks remain unchanged. Rh/Al, O/Al and C/Al XPS atomic ratios, remained unchanged during H_2 treatment, CO_2 introduction or after reaction at 298 K. No significant increase in the carbon content was observed after reaction. There is no effect of the temperature of the catalytic test. The same results were obtained for the two other temperatures (373 and 423 K).

CO_2 chemisorption experiments show that the amount of carbon dioxide adsorbed on the fresh Rh/γ-Al_2O_3 catalyst is very low. However when the catalyst is reduced after hydrogen treatment, the amount of adsorbed carbon dioxide is higher (Fig. 3). The average of CO_2 adsorbed on Rh/γ-Al_2O_3 is 0.12 cm^3/g and this value is equal to 1.28 cm^3/g for the reduced catalysts, namely, the amount of CO_2 adsorbed is 10 times higher for the reduced catalyst.

4. Discussion

Results show that at low temperature (298 K), it is possible to obtain CH_4 when putting in contact CO_2 and H_2 in the presence of a particular catalyst, Rh/γ-Al_2O_3. In these experiments, methane is the only hydrocarbon product which was observed in mass spectrometry analysis. No other species (like ethane, propane, ethane, propylene, butane, butene, methanol, formaldehyde) was been observed during the catalytic test. The temperature also influences the production of methane (Table 1). The amount of CH_4 produced is higher further to an increase of the reaction temperature. Table 1 shows the amount of CH_4 produced expressed in $mol_{CH_4}\ mol^{-1}_{Rh(s)}\ h^{-1}$ and discards the possibility of a stoichiometry conversion between Rh and methane: each Rh atom is shown to operate several catalytic cycles.

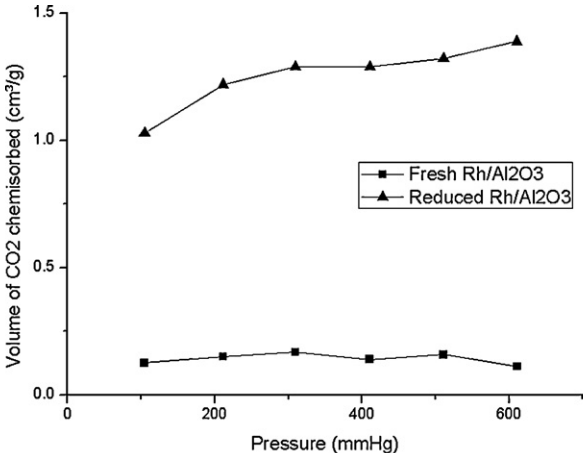

Fig. 3. Chemisorption of carbon dioxide on the fresh catalyst without reduction and on the reduced catalyst.

The results show that no production of CH_4 has been observed when the fresh catalyst was used without reduction (Table 1). The amount of CO_2 chemisorbed (Fig. 3) is very low. The quantity of CO_2 chemisorbed is significantly higher when the reduced catalyst was used. In this case, an important production of methane was observed. This suggests that the first step of the mechanism in the methanation reaction could be the chemisorption of CO_2 on the catalysts. The second step is the dissociative adsorption of CO_2 to form $CO_{(ads)}$ and $O_{(ads)}$ species adsorbed on the surface of the reduced catalyst.

The dissociative adsorption of CO_2 into carbon monoxide and oxygen on the surface of the catalyst has been evidenced by *in situ* DRIFT experiments. The formation of $CO_{(ads)}$ is indeed confirmed on the surface of the Rh/γ-Al_2O_3 by the presence of the bands which correspond to Rh–CO, Rh^{3+}–CO and Rh–$(CO)_2$. The bands related to gem-dicarbonyl and CO associated with an oxidized Rh, react rapidly with hydrogen. The fact that Rh is oxidized during the reaction seems to confirm that CO_2 is dissociated on the surface of the catalyst. The catalyst is oxidized by the dissociated $O_{(ads)}$ species [18,19].

The reduction under hydrogen is an important step to improve the catalytic activity. The reduced rhodium species seems to play an important role in the reaction mechanism. An oxidation of rhodium is observed during the reaction and this is correlated to the deactivation of the catalyst.

Another important observation is the oxidant role of dissociated $O_{(ads)}$. The oxidizing role of CO_2 has been demonstrated previously [18,19]. It has then been suggested that the dissociated $O_{(ads)}$ species are responsible for the oxidation of both the reduced oxide and the hydrocarbons during partial oxidation reactions. In these cases, it has been established that the catalysts work in a higher oxidation state when CO_2 is present. The present results confirm the previous ones. It could be suggested that dissociated $O_{(ads)}$ is responsible for the oxidation of Rh during methanation.

When a high amount of CO_2 was introduced into the reactor (many cycles, Fig. 1), the catalyst was deactivated, probably

Table 3
XPS analysis of alumina and of fresh, after reduction, and after reaction with H_2 on Rh/γ-Al_2O_3 catalysts.

	C/Al	Rh/Al	O/Al	BE Al 2p (eV)	BE Rh $3d_5$ (eV)	BE O 1s (eV)
γ-Al_2O_3	0.2	–	1.5	74.5	–	531.1
Rh/γ-Al_2O_3	0.4	0.01	1.5	74.5	310.1	531.1
Rh/γ-Al_2O_3 after reduction	0.4	0.01	1.4	74.6	307.9	531.1
Rh/γ-Al_2O_3 after reaction	0.5	0.01	1.3	74.7	308.4	531.2

BE: binding energies and Rh/Al, C/Al and O/Al XPS: atomic ratio.

due to an oxidation of Rh by CO_2, more precisely by the oxygen species. When a small amount of CO_2 was introduced on the catalyst (Table 1), the rate of methanation is higher. When a high amount of CO_2 is fed, catalysts lose their activity because they are oxidized. Methane production from CO_2 and H_2 at low temperature and atmospheric pressure can be seriously envisaged at present but optimization is mandatory to minimize the catalyst deactivation by the rhodium oxidation.

5. Conclusion

The mechanism by which methane is produced is the dissociative adsorption of CO_2 on the surface of Rh/γ-Al_2O_3 catalyst. The first step of the methanation reaction could be the chemisorption of CO_2 on the catalysts. The second step is the dissociation of CO_2 into CO and O adsorbed on the surface. The third step is the reaction of dissociated species with hydrogen. The adsorption of CO_2 can be improved by the catalyst reduction: CO_2 oxidizes the catalysts. CO_2 adsorbed as gem-dicarbonyl and CO associated with oxidized Rh are the most reactive species with hydrogen.

Up to now, the mechanism by which the hydrogen reacts with the dissociated species is not determined. Experiments must be done to clarify the next steps of the reaction. It has been suggested that $CO_{(ads)}$ is dissociated into C and O on the surface of the catalysts and that C could react with H_2 and produce CH_4 [20]. Another hypothesis is the formation of CH_4 from CO_2 and H_2 following a Fisher-Tropsch reaction [21]. No experimental arguments to discriminate between these mechanisms were obtained.

These results confirm previous results, namely that it is possible to produce methane via an exclusively inorganic way at room temperature [12]. The formation of CH_4 at such low temperature is a breakthrough in the knowledge of the role and in the use of CO_2. Methane is the raw material for the production of many hydrocarbons but an optimization of the performances of the catalyst and of the reaction conditions must be carried out.

Acknowledgments

The authors gratefully acknowledge the financial support of the Belgium National Fund for Scientific Research (FSR-FNRS), of CGRI (Belgium) and of DGRTE-RW (Belgium). They also wish to thank the Belgian Science Policy: Interuniversity attraction pole (IAP), phase VI, “Advanced complex inorganic materials by a novel bottom-up nanochemistry approach: processing and shaping (INANOMAT)” for the financial support of students and researchers exchanges. M. Jacquemin is grateful to the FRIA for a PhD Student position. The authors also acknowledge the FNRS (Belgium) for the acquisition of the XPS equipment. The authors acknowledge Pr. D. Duprez and Dr. N. Bion from the University of Poitiers for the insightful discussion about the results.

References

[1] M. Aresta, A. Dibenedetto, Catal. Today 98 (2004) 455–462.
[2] J.T. Litynski, S.M. Klara, H.G. McIlvried, R.D. Srivastava, Environ. Int. 32 (2006) 128–144.
[3] J.D. Sharp, M.K. Jaccard, D.W. Keith, Int. J. Greenhouse Gas Control 3 (2009) 641–651.
[4] C. Song, Catal. Today 115 (2006) 2–32.
[5] P. Lunde, F. Kester, Ind. Eng. Chem. Proc. Des. Dev. 13 (1974) 27–33.
[6] F.-W. Chang, T.-J. Hsiao, S.-W. Chung, J.-J. Lo, Appl. Catal. A 164 (1997) 225–236.
[7] F.J. Pérez-Alonso, M. Ojeda, T. Herranz, S. Rojas, J.M. González-Carballo, P. Terreros, J.L.G. Fierro, Catal. Commun. 9 (2008) 1945–1948.
[8] J.J. Spivey, E.M. Wilcox, G.W. Roberts, Catal. Commun. 9 (2008) 685–689.
[9] D.R. Burri, K.-M. Choi, S.-C. Han, A. Burri, S.-E. Park, J. Mol. Catal. A: Chem. 269 (2007) 58–63.
[10] S.T. Srimat, C.S. Song, ACS Symposium Series, vol. 809, 2002, pp. 289–302 (Chapter 19).
[11] L.H. Dubois, G.A. Samorjai, Surf. Sci. 128 (1983) 231–235.
[12] P. Ruiz, M. Jacquemin, N. Blangenois, Patent WO 2010006386 (2010).
[13] N.Z. Muradov, T.N. Veziroglu, Int. J. Hydrogen Energy 33 (2008) 6804–6839.
[14] A. Ishikawa, E. Iglesia, J. Catal. 252 (2007) 49–56.
[15] J. Haber, M. Nattich, T. Machej, Appl. Catal. B 77 (2008) 278–283.
[16] D. Duprez, J. Barrault, C. Geron, Appl. Catal. 37 (1988) 105–114.
[17] D.C. Tomczak, G.D. Lei, V. Schunemann, H. Trevino, W.M.H. Sachtler, Micropor. Mater. 5 (1996) 263–278.
[18] F. Dury, E.M. Gaigneaux, P. Ruiz, Appl. Catal. A 242 (2003) 187–203.
[19] C. Cellier, D. Le Clef, C. Mateos-Pedrero, P. Ruiz, Catal. Today 106 (2005) 47–51.
[20] M. Gratzel, J. Kiwi, K.R. Thampi, US Patent 4,847,231 (1989).
[21] T. Riedel, M. Claeys, H. Schulz, G. Schaub, S.-S. Nam, K.-W. Jun, M.-J. Choi, G. Kishan, K.-W. Lee, Appl. Catal. A 186 (1999) 201–213.